Supplement of Biogeosciences, 22, 1393–1411, 2025
https://doi.org/10.5194/bg-22-1393-2025-supplement
© Author(s) 2025. CC BY 4.0 License.

Biogeosciences Open Access EGU

Supplement of

Impact of winter warming on CO_2 fluxes in evergreen needleleaf forests

Mana Gharun et al.

Correspondence to: Mana Gharun (mana.gharun@wwu.de)

The copyright of individual parts of the supplement might differ from the article licence.

Supplementary Material
Impact of Winter Warming on CO_2 Fluxes in Evergreen Needle-Leaf Forests

Table S1 Mean seasonal NEP (µmol CO_2 m^{-2} s^{-1}) during 2020 compared to the reference period (2014-2019). Negative values indicate a net CO_2 emission and positive values indicate a net CO_2 uptake.

	NEP - winter		**NEP- spring**		**NEP - summer**		**NEP - autumn**	
Site	Reference	2020	Reference	2020	Reference	2020	Reference	2020
IT-SR2	-0.18	0.63	2.03	2.33	0.82	1.53	-0.71	-0.71
FR-Bil	0.21	0.16	2.38	1.94	1.17	2.04	-0.08	0.51
BE-Bra	-1.39	-2.79	1.41	1.10	3.42	2.46	-0.34	-1.35
DE-Tha	-0.22	-0.18	2.07	1.83	2.48	1.28	0.70	0.50
DE-RuW	1.53	1.23	2.69	2.21	0.96	-0.01	0.84	0.70
DE-Obe	-1.25	-1.56	2.21	1.49	2.10	0.88	-0.44	-0.14
SE-Nor	-1.42	-1.29	0.58	0.87	-0.01	0.18	-2.51	-2.57
CZ-Bk1	-0.36	-0.30	3.59	2.25	3.78	-0.01	1.48	0.38
RU-Fyo	-0.63	-0.55	0.76	1.55	0.86	0.55	-0.70	-0.45
FI-Let	-0.78	-1.05	0.01	0.49	0.88	1.84	-1.26	-1.32
IT-Ren	-0.38	-0.61	2.38	3.04	3.58	2.86	1.47	1.47
CH-Dav	-1.34	-1.29	1.38	1.21	1.20	0.18	0.29	-0.34
SE-Ros	-0.37	-0.35	1.02	0.69	2.19	1.95	-0.07	-0.57
SE-Svb	-0.64	-0.69	1.12	0.54	2.04	2.41	-0.80	-0.78

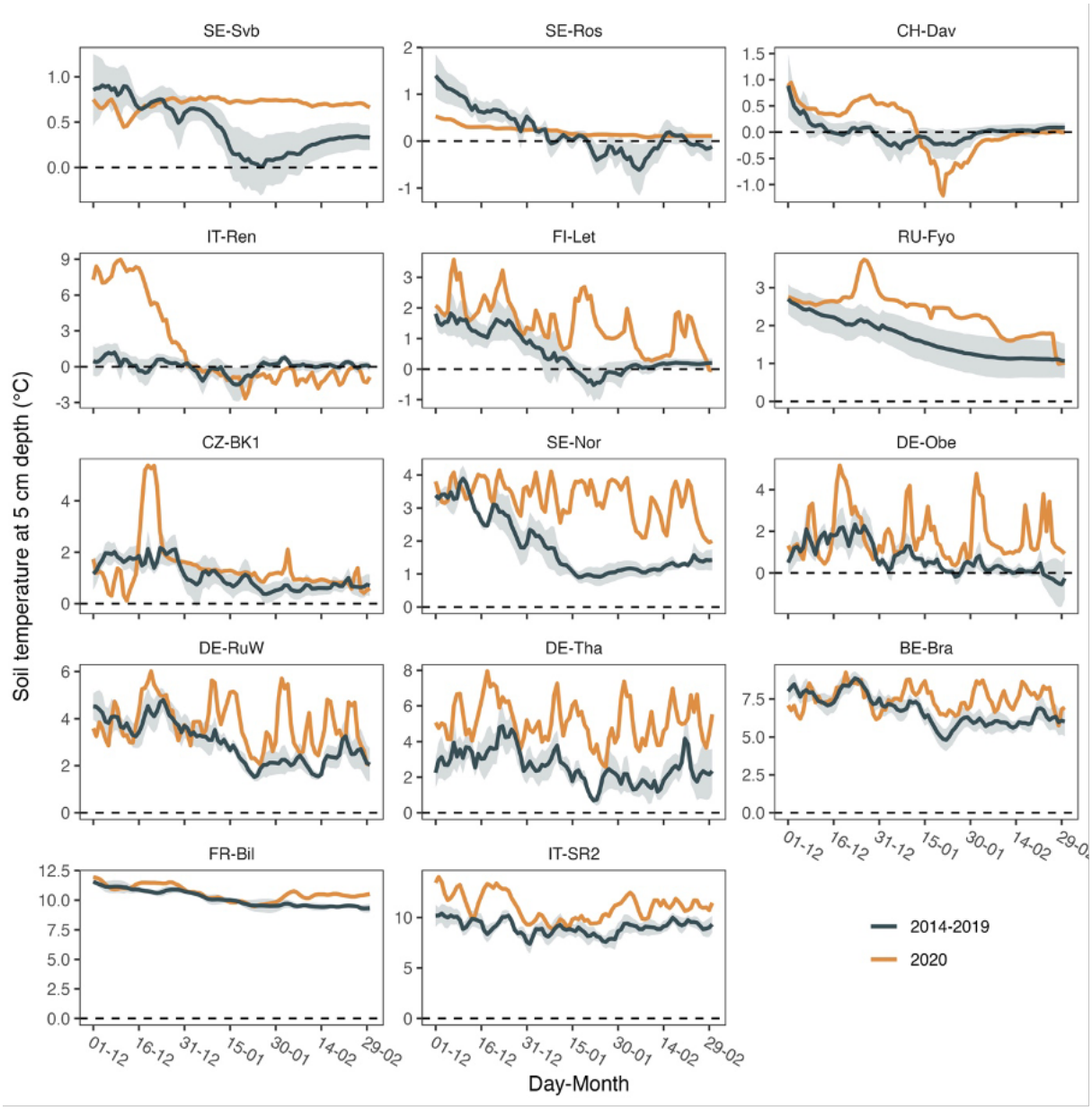

Figure S1 Soil temperature (at 5cm) changes in winter 2020 compared to the winter of the reference period (2014-2019). Shaded bands around the mean show the 95% confidence interval (CI) of mean soil temperature. Sites are ordered (top and left to right) by increasing site mean temperature (SE-Svb coldest and IT-SR2 warmest).

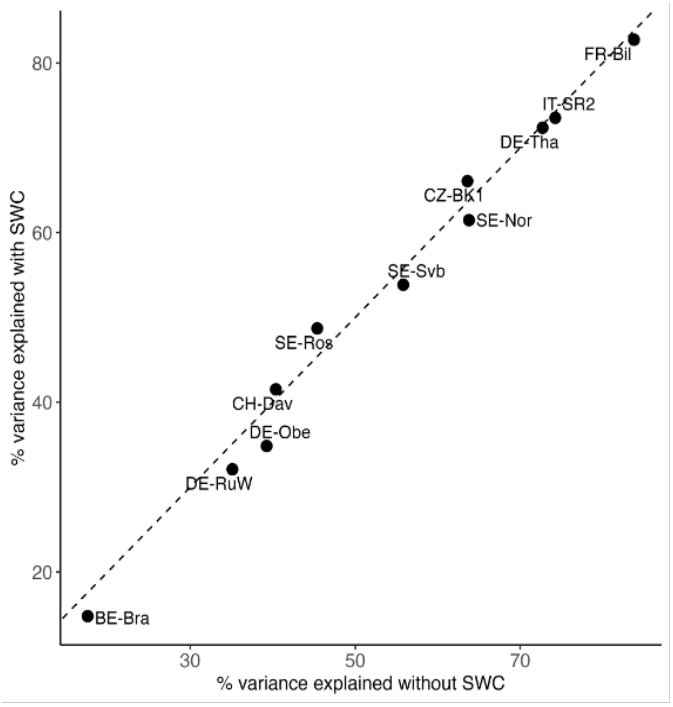

Figure S2 Comparison of the percentage of variance explained by the random forest model, with and without the inclusion of soil water content (SWC) across 11 sites where SWC measurements were available. The dashed line represents the 1:1 reference line.

a)

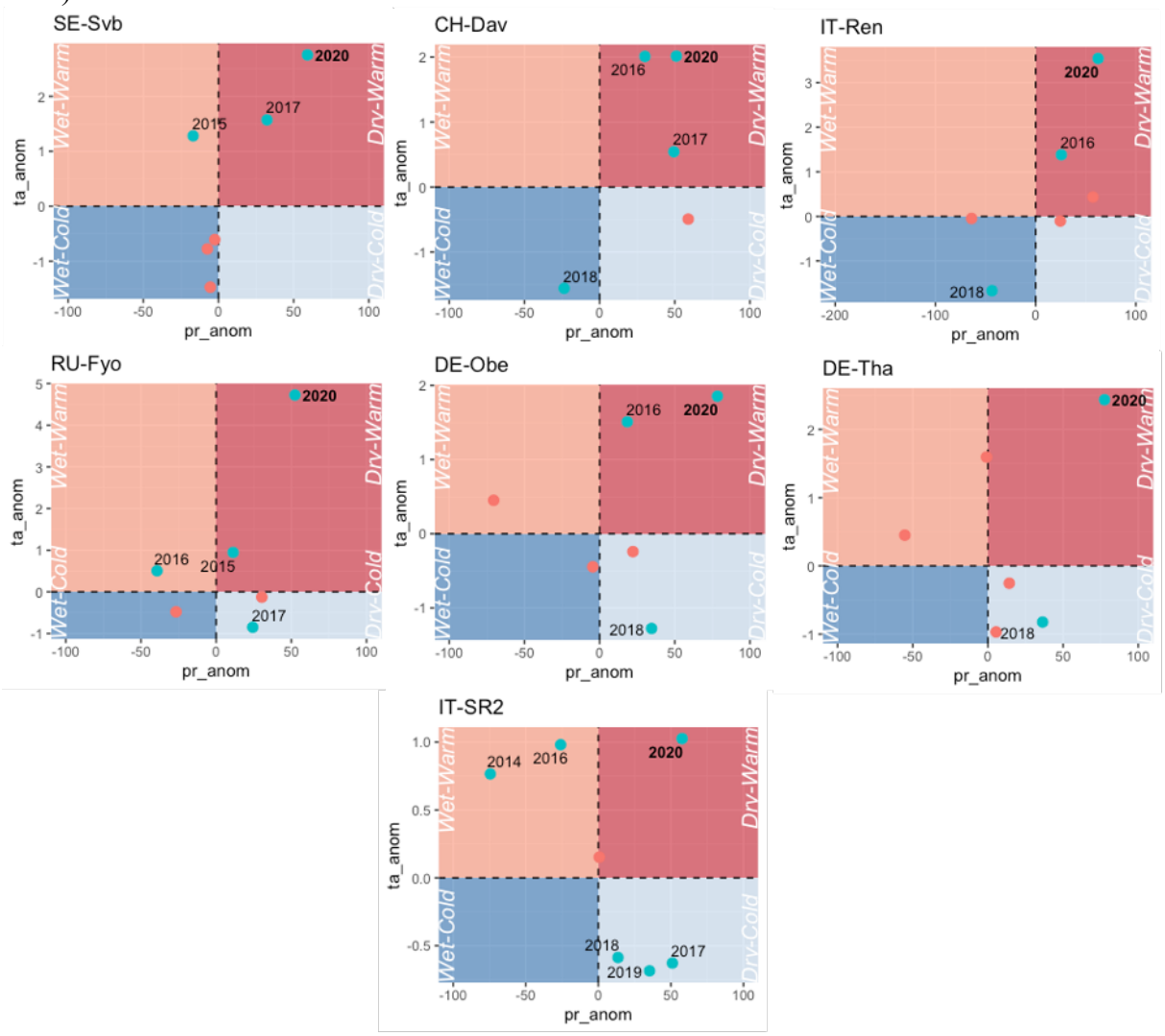
SE-Svb
CH-Dav
IT-Ren
RU-Fyo
DE-Obe
DE-Tha
IT-SR2
Wet-Warm
Dry-Warm
Wet-Cold
Dry-Cold
ta_anom
pr_anom
2020
2017
2015
2016
2018
2014
2019

b)

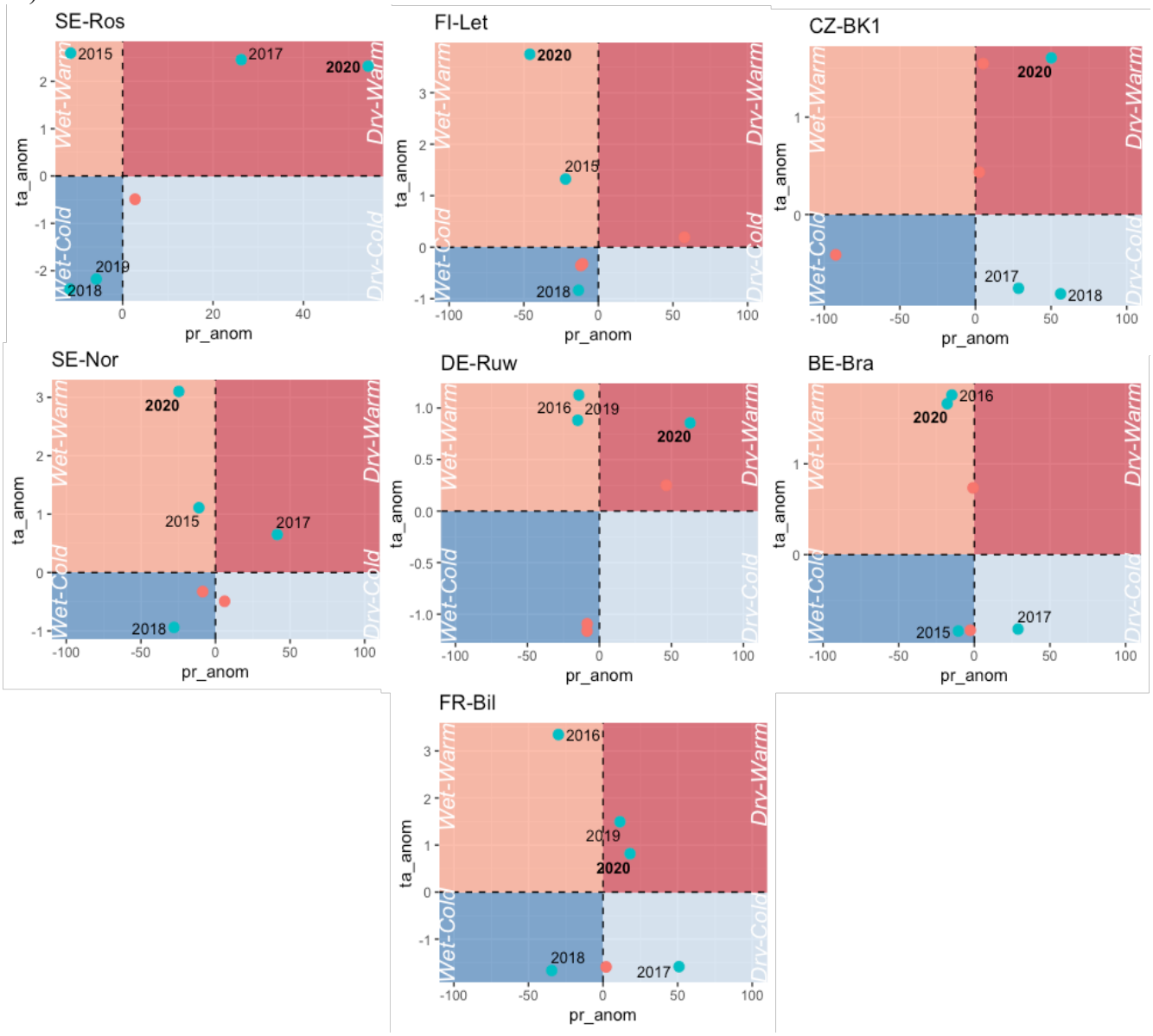

Figure S3 Winter temperature anomalies (ta_anom = ta - ta_mean) and precipitation anomalies translated to dryness as: pr_anom = ((pr/pr_mean)*100-100)*(-1) in winter 2020 relative to winter during the reference period 2014-2019 at: a) the sites where winter 2020 was the warmest and driest winter, and b) at the remaining sites. Precipitation anomalies were converted to relative change (relative to mean) and temperature changes are presented in the original unit (°C). Anomalies are classified in four main classes of "wet-warm", "dry-warm", "wet-cold", and "dry-cold". Winter 2020 is marked in bold. Symbols are marked in blue, and label (year) is displayed only if precipitation anomaly was larger than 10% and at the same time temperature change was more than 0.5 °C. Sites are ordered in each panel by increasing mean temperature.

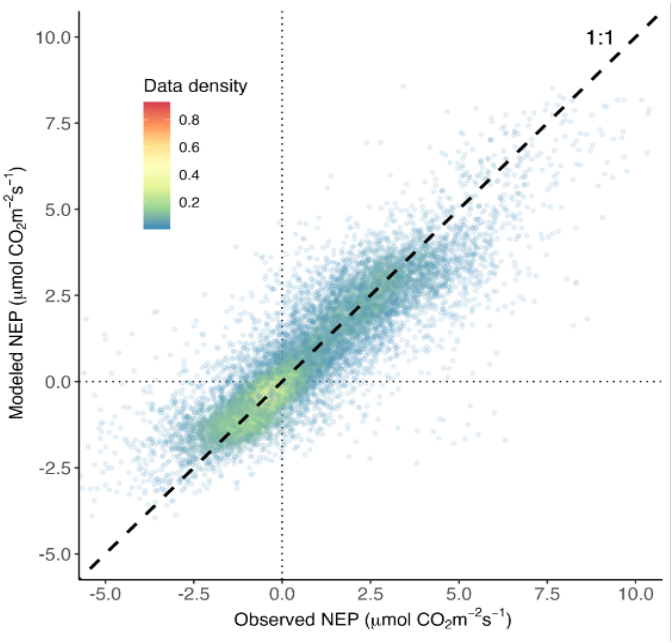

Figure S4 Density scatter plot showing the performance of the random forest regression model of NEP. The average variance explained (across all sites) by the random forest model was 78% ($r^2 = 0.78$).

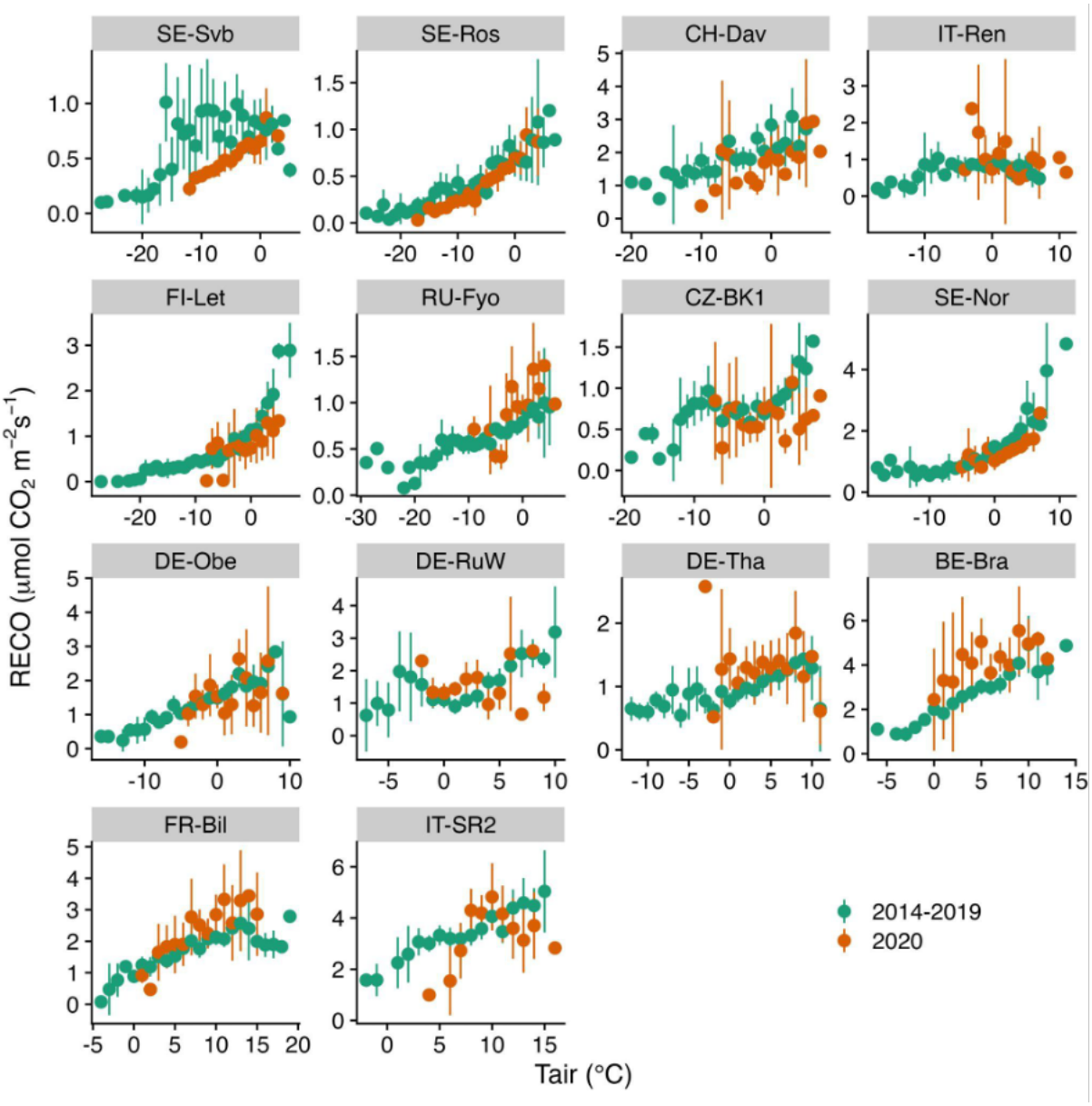

Figure S5 Comparison of Reco vs Tair (air temperature) binned response during the winter of the reference period (2014-2019) and 2020 winter, across all sites (arranged from top to bottom based on increasing site mean air temperature). The daily mean Reco is aggregated (mean ± 95% CI as error bars) at 1°C Tair bins.

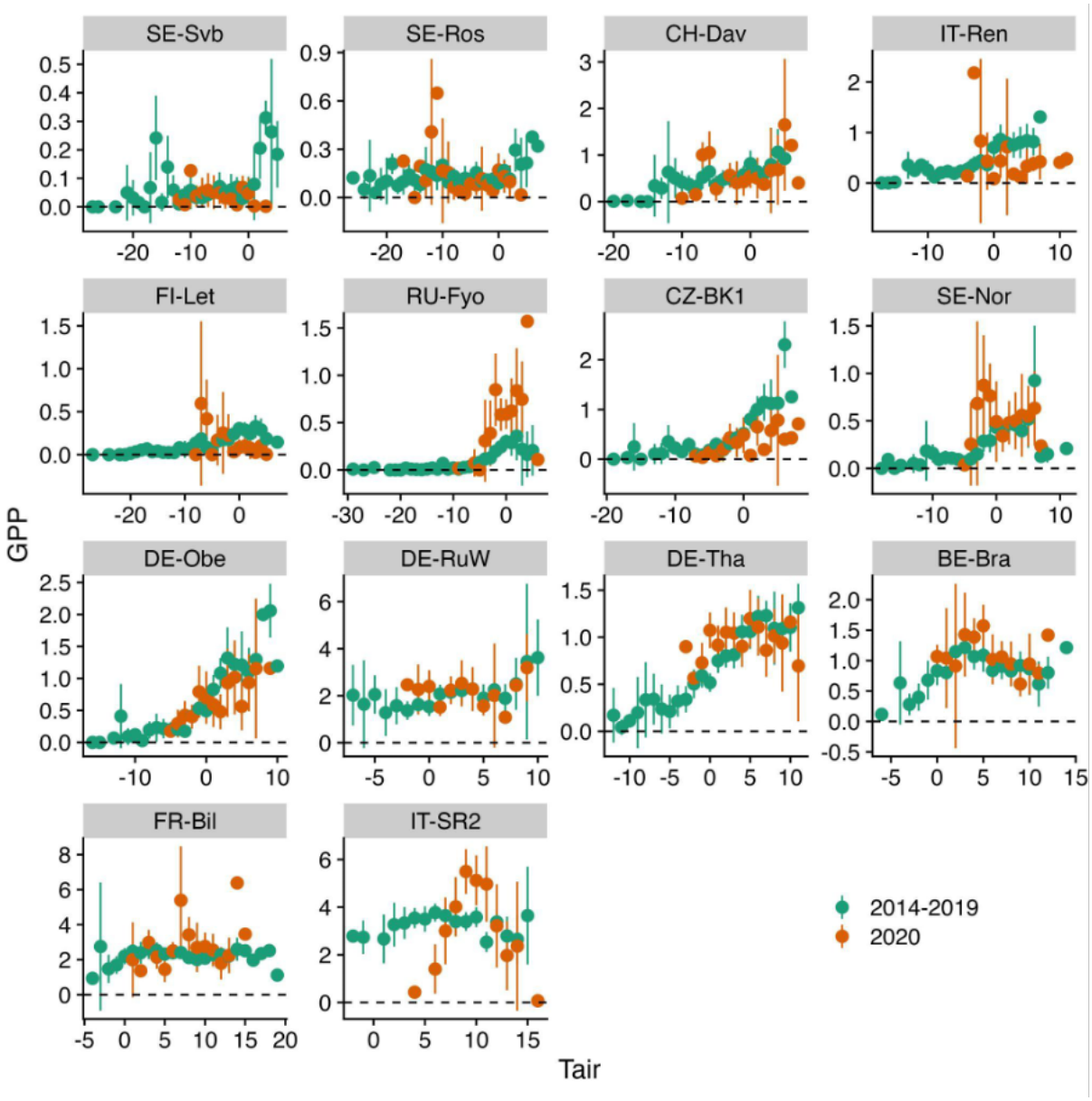

Figure S6 Comparison of GPP vs Tair (air temperature) binned response during the winter of the reference period (2014-2019) and winter 2020 across all sites (arranged from top to bottom based on increasing mean air temperature). The daily mean GPP is aggregated (mean ± 95% CI as error bars) at 1°C Tair bins.

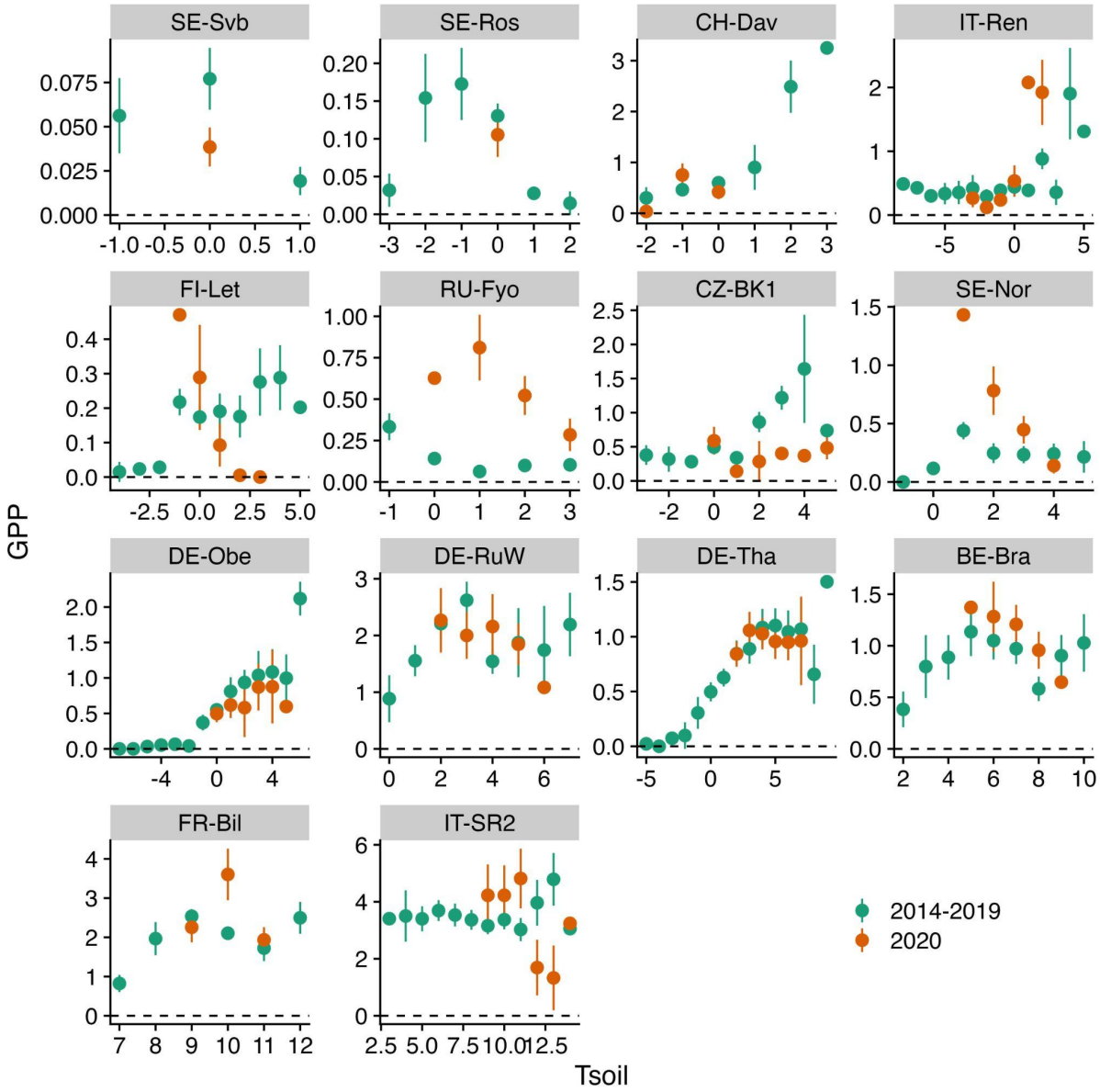

Figure S7 Comparison of GPP vs Tsoil (soil temperature) binned response during the winter of the reference period (2014-2019) and winter 2020 across all sites (arranged from top to bottom based on increasing mean air temperature). The daily mean GPP is aggregated (mean ± 95% CI as error bars) at 1°C Tsoil bins.

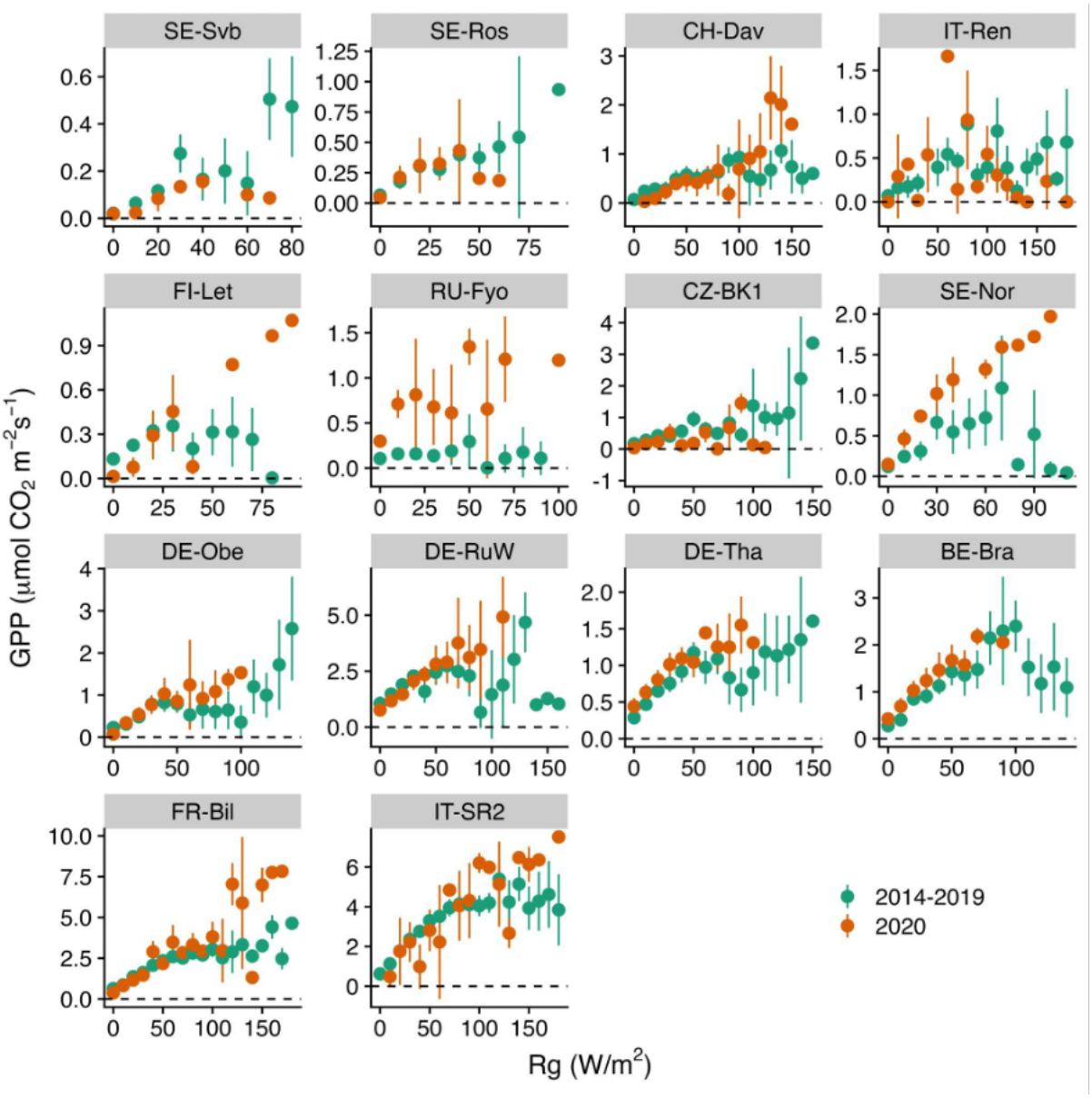

Figure S8 Comparison of GPP vs Rg (incoming shortwave radiation) binned response during the winter of the reference period (2014-2019) and winter 2020 across all sites (arranged from top to bottom based on increasing mean air temperature). The daily mean GPP is aggregated (mean ± 95% CI as error bars) at 10 Wm^{-2} Rg bins.

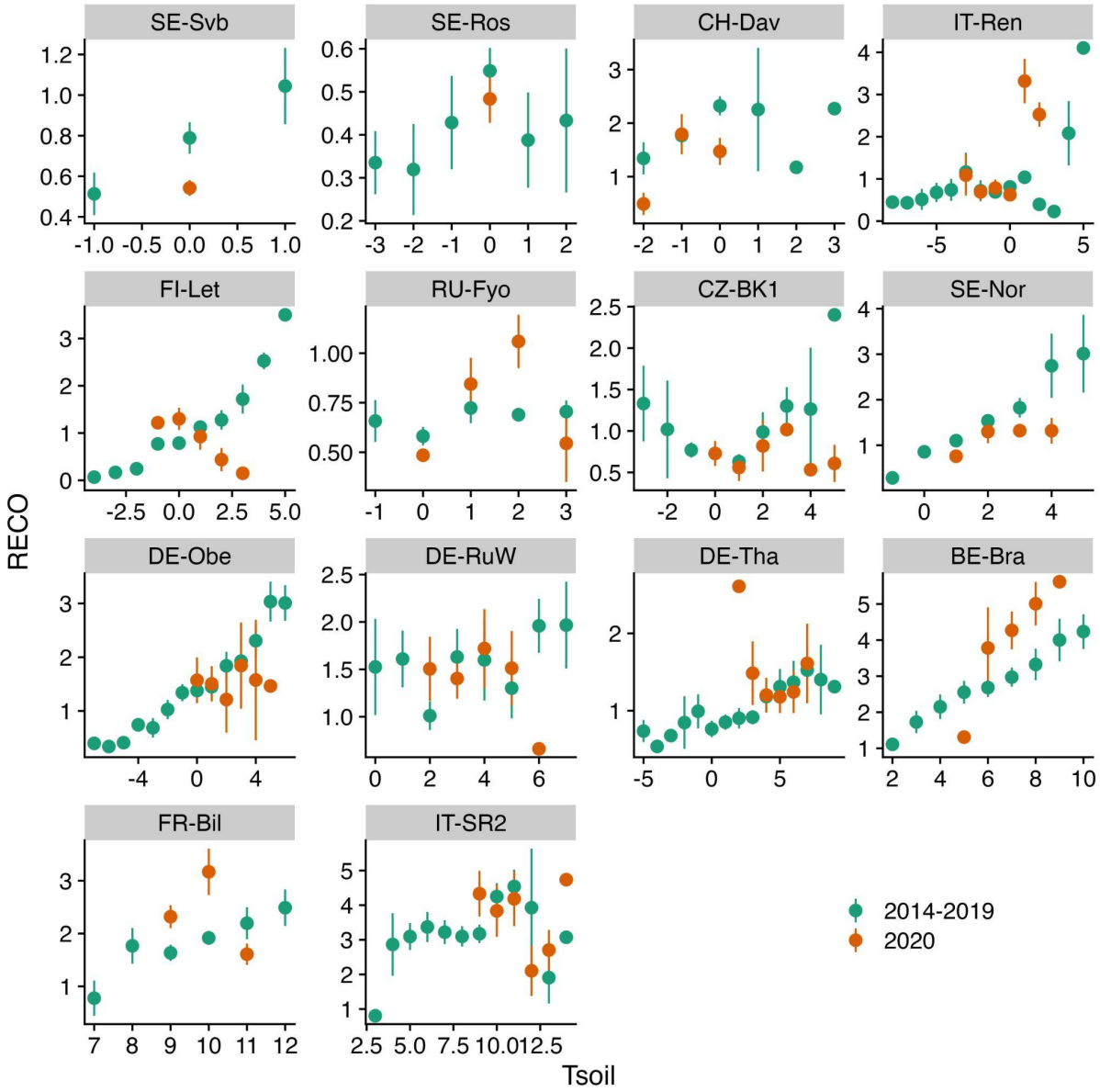

Figure S9 Comparison of Reco vs Tsoil (soil temperature) binned response during the winter of the reference period (2014-2019) and winter 2020 across all sites (arranged from top to bottom based on increasing mean air temperature). The daily mean Reco is aggregated (mean ± 95% CI as error bars) at 1°C Tsoil bins.

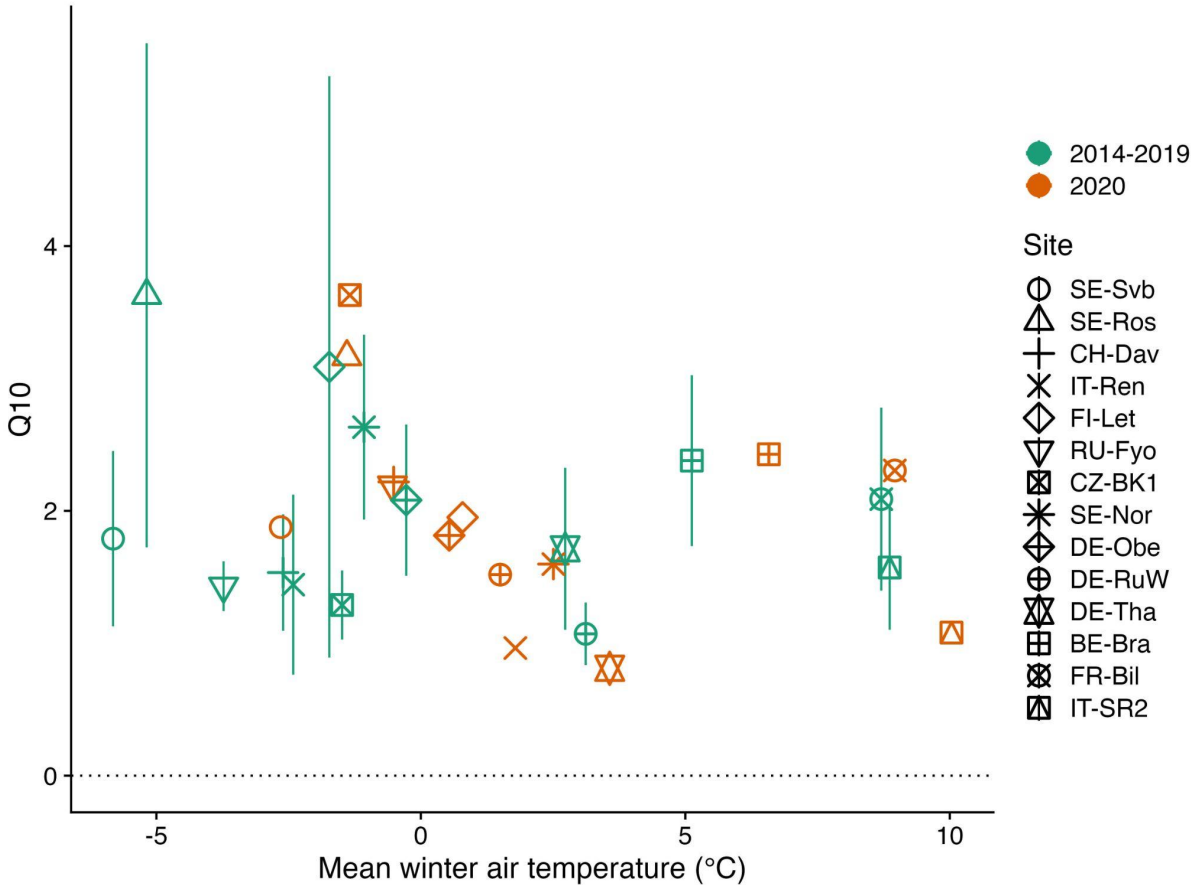

Figure S10 The temperature sensitivity of ecosystem respiration (Q10) during winter for the reference period (2014-2019) and in winter 2020 across all sites. Q10 was calculated for each winter year from 2014 to 2022. The reference (2014-2019) is represented as mean and 95% CI (as error bars).

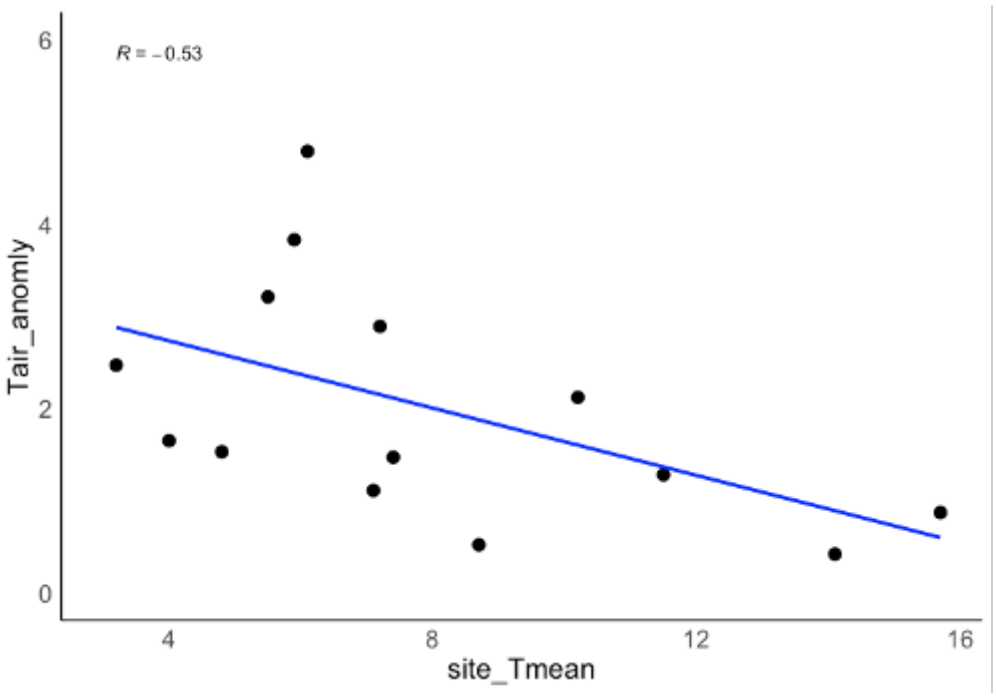

Figure S11 The relationship between site mean air temperature and air temperature anomalies observed in winter 2020 was significant ($p < 0.05$)